

# Synthesis and Characterization of $(\mu\text{-H})_2\text{Os}_3(\text{CO})_9(\text{PPh}_3)(\mu\text{-CH}_2)$ and Related Compounds. Phosphine Ligand Effects on the Methylene/Methyl Tautomerization

David H. Hamilton and John R. Shapley\*

Department of Chemistry, University of Illinois, Urbana, Illinois 61801

Received June 4, 1999

Treatment of the phosphine ligand derivatives  $(\mu\text{-H})_2\text{Os}_3(\text{CO})_9\text{L}$  ( $\text{L} = \text{PEt}_3$ ,  $\text{PEt}_2\text{Ph}$ ,  $\text{PPh}_3$ ,  $\text{PiPrPh}_2$ ,  $\text{PCy}_3$ ) with excess ethereal diazomethane at  $-78^\circ\text{C}$  provides a set of compounds with the formula  $\text{Os}_3(\text{CO})_9\text{L}(\text{CH}_4)$ . As isolated solids these compounds exist as methylene ligand complexes, and the structure of  $(\mu\text{-H})_2\text{Os}_3(\text{CO})_9(\text{PPh}_3)(\mu\text{-CH}_2)$  has been determined by single-crystal X-ray crystallography. A triangular array of osmium atoms supports a methylene moiety bridging one Os–Os vector, and the triphenylphosphine ligand is bound to the remaining osmium center in an "in-plane" position. The hydride ligands have been located and refined; one also bridges the same edge as the methylene ligand, and the other forms a single bridge in a position cis to the phosphine ligand. Analysis of the solution  $^1\text{H}$  and  $^{13}\text{C}$  NMR spectra of  $(\mu\text{-H})_2\text{Os}_3(\text{CO})_9(\text{PPh}_3)(\mu\text{-CH}_2)$  indicates that the solid-state structure is maintained in solution. However, also present in solution is a methyl tautomer,  $(\mu\text{-H})\text{-Os}_3(\text{CO})_9(\text{PPh}_3)(\mu\text{-CH}_3)$ , the structure of which has been inferred by a combination of spectroscopy, labeling, and reactivity studies as having both the methyl group and the hydride ligand bridging the edge adjacent to the phosphine ligand. For the various derivatives, the equilibrium amount of the methyl tautomer depends strongly on the size of the phosphine ligand, ranging from 1:12 for  $\text{L} = \text{PEt}_3$ , through 1:56 for  $\text{L} = \text{PPh}_3$ , to essentially zero for  $\text{L} = \text{PCy}_3$ . Protonation of  $(\mu\text{-H})_2\text{Os}_3(\text{CO})_9\text{L}(\mu\text{-CH}_2)$  ( $\text{L} = \text{PPh}_3$ ,  $\text{PCy}_3$ ) occurs at an Os–C bond of the methylene ligand to produce a cationic methyl compound. In this case the methyl group bridges the same edge as in the methylene precursor: that is, a position remote from the phosphine ligand. Pyrolysis of  $(\mu\text{-H})_2\text{Os}_3(\text{CO})_9(\text{PPh}_3)(\mu\text{-CH}_2)$  in refluxing toluene forms the methylidyne derivative  $(\mu\text{-H})_3\text{Os}_3(\text{CO})_8(\text{PPh}_3)(\mu\text{-CH})$  in high yield. The reaction of the methyl/methylene tautomer mixture with ethylene to eliminate methane and form a hydrido vinyl compound shows a strong dependence on the size of the phosphine ligand, with inhibition by bulkier ligands. However, the action of the tautomer mixture to catalyze the decomposition of excess diazomethane into nitrogen and a hydrocarbon polymer depends on the electronic properties of the phosphine ligand, with stronger donors showing slower rates.

## Introduction

The reaction between  $(\mu\text{-H})_2\text{Os}_3(\text{CO})_{10}$  and diazomethane affords  $\text{Os}_3(\text{CO})_{10}(\text{CH}_4)$  (**1**), which is isolated as the methylene compound  $(\mu\text{-H})_2\text{Os}_3(\text{CO})_{10}(\mu\text{-CH}_2)$  (**1a**) but exists in solution as a 3:1 mixture with the methyl tautomer  $(\mu\text{-H})\text{Os}_3(\text{CO})_{10}(\mu\text{-CH}_3)$  (**1b**).<sup>1,2</sup> The reactivity of the **1a/1b** mixture depends on the presence of both forms: (i) when it is heated, carbon monoxide is lost and the methylidyne complex  $(\mu\text{-H})_3\text{Os}_3(\text{CO})_9(\mu\text{-CH})$  is formed; (ii) when it is treated with incipient ligands, methane is lost and new complexes are formed (see Scheme 1). In the specific case of ethylene, the product isolated is the hydrido vinyl complex  $(\mu\text{-H})\text{Os}_3(\text{CO})_{10}$

( $\mu\text{-CH=CH}_2$ ), which is also formed by the reaction of  $(\mu\text{-H})_2\text{Os}_3(\text{CO})_{10}$  with both acetylene<sup>3</sup> and ethylene.<sup>4</sup> A phosphine ligand substituted precursor,  $(\mu\text{-H})_2\text{Os}_3(\text{CO})_9\text{L}$ , has been used in a variety of reactions to probe the effects of ligand electronic and steric asymmetry on the derivatives formed.<sup>5</sup> We now report the new set of compounds  $\text{Os}_3(\text{CO})_9\text{L}(\text{CH}_4)$ , prepared from  $(\mu\text{-H})_2\text{Os}_3(\text{CO})_9\text{L}$  and diazomethane. The compounds are isolated as the methylene ligand complexes  $(\mu\text{-H})_2\text{Os}_3(\text{CO})_9\text{L}(\mu\text{-CH}_2)$  ( $\text{L} = \text{PEt}_3$  (**2a**),  $\text{PEt}_2\text{Ph}$  (**3a**),  $\text{PPh}_3$  (**4a**),  $\text{PiPrPh}_2$  (**5a**),  $\text{PCy}_3$  (**6a**)). However, we show that a methyl tautomer analogous to **1b** also exists in solution to an extent that decreases with increasing effective size of the phosphine ligand. More bulky ligands also inhibit the reaction of these compounds with ethylene, but their activity as catalysts for the decomposition of excess

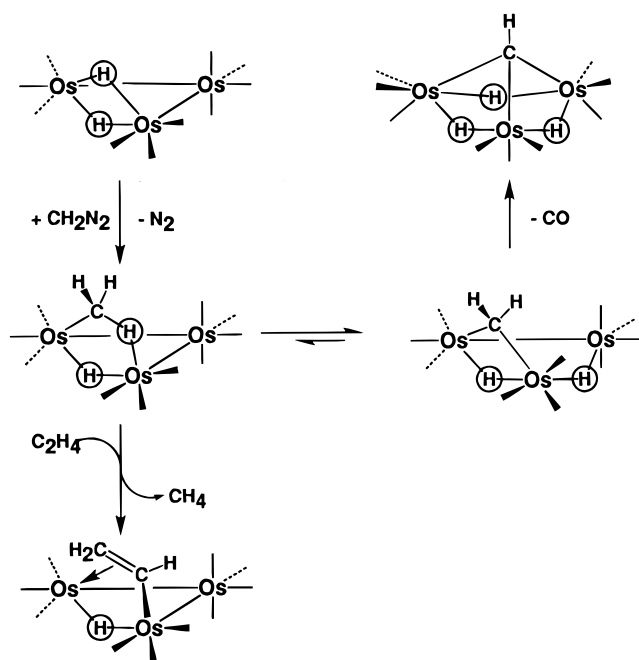
(1) (a) Calvert, R. B.; Shapley, J. R. *J. Am. Chem. Soc.* **1978**, *100*, 7726. (b) Calvert, R. B.; Shapley, J. R. *J. Am. Chem. Soc.* **1977**, *99*, 5225. (c) Calvert, R. B. Ph.D. Thesis, University of Illinois, Urbana, IL, 1979.

(2) (a) Schultz, A. J.; Williams, J. M.; Calvert, R. B.; Shapley, J. R.; Stucky, G. D. *Inorg. Chem.* **1979**, *18*, 319. (b) Calvert, R. B.; Shapley, J. R.; Schultz, A. J.; Williams, J. M.; Suib, S. L.; Stucky, G. D. *J. Am. Chem. Soc.* **1978**, *100*, 6240.

(3) Deeming, A. J.; Underhill, M. *J. Chem. Soc., Dalton Trans.* **1974**, 1415.

(4) (a) Keister, J. B.; Shapley, J. R. *J. Organomet. Chem.* **1975**, *85*, C29. (b) Cree-Uchiyama, M.; Shapley, J. R.; St. George, G. M. *J. Am. Chem. Soc.* **1986**, *108*, 1316.

Scheme 1



diazomethane depends instead on the relative donor properties of the phosphine ligand.

### Experimental Section

**General Procedures.** All reactions were carried out under a nitrogen atmosphere. Diethyl ether was distilled from sodium/benzophenone. Dichloromethane was distilled from calcium hydride. *p*-Xylene (Aldrich) was used as received. Ethereal diazomethane was prepared from Diazald (Aldrich) according to the literature procedures<sup>6</sup> and then stored over molecular sieves (3 Å). Trifluoroacetic acid, trifluoroacetic acid-*d*, tetrafluoroboric acid, and *tert*-butyl isocyanide were purchased from Aldrich and used without further purification. The compounds  $(\mu\text{-H})_2\text{Os}_3(\text{CO})_9\text{L}$  were prepared by literature methods.<sup>7</sup> The labeled compound  $(\mu\text{-D})_2\text{Os}_3(\text{CO})_{10}$  was prepared analogously to  $(\mu\text{-H})_2\text{Os}_3(\text{CO})_{10}$  by using deuterium (Air Products, 99%) instead of hydrogen.<sup>8</sup> Triosmium dodecacarbonyl was enriched in  $^{13}\text{C}$  (ca. 50%) by heating a Decalin solution at 120 °C for 3 days in the presence of an atmosphere of  $^{13}\text{CO}$  (Isotec, 99%).  $^1\text{H}$  NMR spectra were recorded at 499.696 MHz on a Unity 500 Varian spectrometer. Infrared spectra were obtained on a Perkin-Elmer 1750 FT-IR spectrometer. Elemental analyses were performed by the staff of the Microanalytical Laboratory of the School of Chemical Sciences, and mass

spectra were obtained by the staff of the School Mass Spectrometry Laboratory.

**Preparation of  $\text{Os}_3(\text{CO})_9(\text{PPh}_3)(\text{CH}_4)$  (4).** A sample of  $(\mu\text{-H})_2\text{Os}_3(\text{CO})_9\text{PPh}_3$  (100 mg, 0.092 mmol) was dissolved in diethyl ether (200 mL) in a 350 mL round-bottom flask equipped with an addition funnel, and the flask was cooled to  $-78^\circ\text{C}$  with a dry ice–acetone bath. An excess of ethereal diazomethane placed in the addition funnel was added dropwise to the flask with stirring. The mixture was stirred for an additional 20 min; then the cooling bath was removed, and the flask was warmed to room temperature. The resulting dark yellow solution was filtered to remove polymethylene, and the solvent was removed under reduced pressure. The residue was subjected to thin-layer chromatography ( $\text{SiO}_2$ , *n*-hexane), and the major yellow band that developed was extracted with dichloromethane. Evaporation of the solvent and recrystallization of the residue from *n*-pentane yielded the compound as a bright yellow powder (78 mg, 0.071 mmol, 77%). Anal. Calcd for  $\text{C}_{28}\text{H}_{19}\text{O}_9\text{Os}_3\text{P}$ : C, 30.55; H, 1.74. Found: C, 30.58; H, 1.82. IR ( $\text{C}_6\text{H}_{12}$ ):  $\nu(\text{CO})$  2091 w, 2072 w, 2047 m, 2032 w, 2007 vs, 1993 sh, 1977 w, 1969 w  $\text{cm}^{-1}$ .  $^1\text{H}$  NMR ( $\text{CDCl}_3$ ): **4a**,  $\delta$  5.08 (m,  $\text{H}_a$ ), 4.26 (dt,  $\text{H}_b$ ),  $-15.37$  (s, br,  $\text{H}_c$ ),  $-20.18$  (m,  $\text{H}_d$ ),  $J_{aP}$  2.5 Hz,  $J_{ab}$  6.5 Hz,  $J_{ac}$  2.5 Hz,  $J_{ad}$  2.0 Hz,  $J_{bP}$  2.5 Hz,  $J_{bc}$  0.5 Hz,  $J_{bd}$  2.5 Hz,  $J_{cP}$  0.5 Hz,  $J_{cd}$  1.7 Hz,  $J_{dP}$  11.5 Hz; **4b**,  $\delta$   $-3.68$  (s (br),  $\text{H}_a$ ),  $-14.79$  (dq,  $\text{H}_b$ ),  $J_{ab}$  1.0 Hz,  $J_{ap}$  2 Hz,  $J_{bp}$  8 Hz;  $\text{P}(\text{C}_6\text{H}_5)_3$ ,  $\delta$  7.3 (m) and 7.5 (m).

**$\text{Os}_3(\text{CO})_9(\text{PET}_3)(\text{CH}_4)$  (2).** The procedure is analogous to that for **4**. Yield: 52%. Anal. Calcd for  $\text{C}_{16}\text{H}_{19}\text{O}_9\text{Os}_3\text{P}$ : C, 20.08; H, 2.00. Found: C, 20.12; H, 2.10. IR ( $\text{C}_6\text{H}_{12}$ ):  $\nu(\text{CO})$  2090 w, 2068 w, 2042 m, 2029 w, 2000 vs, 1984 m, 1972 w, 1966 w  $\text{cm}^{-1}$ .  $^1\text{H}$  NMR ( $\text{CDCl}_3$ ): **2a**,  $\delta$  5.12 (m,  $\text{H}_a$ ), 4.30 (dt,  $\text{H}_b$ ),  $-15.22$  (s, br,  $\text{H}_c$ ),  $-20.82$  (m,  $\text{H}_d$ ),  $J_{aP}$  2.5 Hz,  $J_{ab}$  6.5 Hz,  $J_{ac}$  2.5 Hz,  $J_{ad}$  2.0 Hz,  $J_{bP}$  2.5 Hz,  $J_{bc}$  0.5 Hz,  $J_{bd}$  2.5 Hz,  $J_{cP}$  0.5 Hz,  $J_{cd}$  1.5 Hz,  $J_{dP}$  9.5 Hz; **2b**,  $\delta$   $-3.65$  (s (br),  $\text{H}_a$ ),  $-14.92$  (dq,  $\text{H}_b$ ),  $J_{ab}$  1.0 Hz,  $J_{ap}$  2 Hz,  $J_{bp}$  8 Hz;  $\text{P}(\text{CH}_2\text{CH}_3)_3$ ,  $\delta$  0.89 (m);  $\text{P}(\text{CH}_2\text{CH}_3)_3$ ,  $\delta$  1.15 (m).

**$\text{Os}_3(\text{CO})_9(\text{PET}_2\text{Ph})(\text{CH}_4)$  (3).** The procedure is analogous to that for **4**. Yield: 55%. Anal. Calcd for  $\text{C}_{20}\text{H}_{19}\text{O}_9\text{Os}_3\text{P}$ : C, 23.90; H, 1.91. Found: C, 24.22; H, 2.02. IR ( $\text{C}_6\text{H}_{12}$ ):  $\nu(\text{CO})$  2090 w, 2066 m, 2042 m, 1998 vs, 1984 m, 1966 w  $\text{cm}^{-1}$ .  $^1\text{H}$  NMR ( $\text{CDCl}_3$ ): **3a**,  $\delta$  5.04 (m,  $\text{H}_a$ ), 4.24 (dt,  $\text{H}_b$ ),  $-15.48$  (s, br,  $\text{H}_c$ ),  $-20.56$  (m,  $\text{H}_d$ ),  $J_{aP}$  2.5 Hz,  $J_{ab}$  6.5 Hz,  $J_{ac}$  2.5 Hz,  $J_{ad}$  2.0 Hz,  $J_{bP}$  2.5 Hz,  $J_{bc}$  0.5 Hz,  $J_{bd}$  2.5 Hz,  $J_{cP}$  0.5 Hz,  $J_{cd}$  1.5 Hz,  $J_{dP}$  9.5 Hz; **3b**,  $\delta$   $-3.65$  (s (br),  $\text{H}_a$ ),  $-14.85$  (dq,  $\text{H}_b$ ),  $J_{ab}$  1.0 Hz,  $J_{ap}$  2 Hz,  $J_{bp}$  8 Hz;  $\text{P}(\text{CH}_2\text{CH}_3)_2(\text{C}_6\text{H}_5)$ ,  $\delta$  0.91 (m);  $\text{P}(\text{CH}_2\text{CH}_3)_2(\text{C}_6\text{H}_5)$ ,  $\delta$  1.19 (m);  $\text{P}(\text{CH}_2\text{CH}_3)_2(\text{C}_6\text{H}_5)$ ,  $\delta$  7.3 (m) and 7.5 (m).

**$\text{Os}_3(\text{CO})_9(\text{PiPrPh}_2)(\text{CH}_4)$  (5).** The procedure is analogous to that for **4**. Yield: 58%. Anal. Calcd for  $\text{C}_{25}\text{H}_{21}\text{O}_9\text{Os}_3\text{P}$ : C, 28.14; H, 1.98. Found: C, 28.37; H, 2.08. IR ( $\text{C}_6\text{H}_{12}$ ):  $\nu(\text{CO})$  2090 w, 2065 m, 2041 m, 1999 vs, 1984 m, 1966 w  $\text{cm}^{-1}$ .  $^1\text{H}$  NMR ( $\text{CDCl}_3$ ): **5a**,  $\delta$  5.03 (m,  $\text{H}_a$ ), 4.26 (dt,  $\text{H}_b$ ),  $-15.53$  (s, br,  $\text{H}_c$ ),  $-20.86$  (m,  $\text{H}_d$ ),  $J_{aP}$  2.5 Hz,  $J_{ab}$  6.5 Hz,  $J_{ac}$  2.5 Hz,  $J_{ad}$  2.0 Hz,  $J_{bP}$  2.5 Hz,  $J_{bc}$  0.5 Hz,  $J_{bd}$  2.5 Hz,  $J_{cP}$  0.5 Hz,  $J_{cd}$  1.5 Hz,  $J_{dP}$  9.5 Hz; **5b**,  $\delta$   $-3.77$  (s (br),  $\text{H}_a$ ),  $-14.89$  (dq,  $\text{H}_b$ ),  $J_{ab}$  1.0 Hz,  $J_{ap}$  2 Hz,  $J_{bp}$  8 Hz;  $\text{P}(\text{C}_6\text{H}_5)_2(\text{CH}(\text{CH}_3)_2)$ ,  $\delta$  0.81 (m);  $\text{P}(\text{C}_6\text{H}_5)_2(\text{CH}(\text{CH}_3)_2)$ ,  $\delta$  1.22 (m);  $\text{P}(\text{C}_6\text{H}_5)_2(\text{CH}(\text{CH}_3)_2)$ ,  $\delta$  7.3 (m) and 7.5 (m).

**$(\mu\text{-H})_2\text{Os}_3(\text{CO})_9(\text{PCy}_3)(\mu\text{-CH}_2)$  (6a).** The procedure is analogous to that for **4**. Yield: 61%. Anal. Calcd for  $\text{C}_{28}\text{H}_{37}\text{O}_9\text{Os}_3\text{P}$ : C, 30.05; H, 3.33. Found: C, 30.18; H, 3.47. IR ( $\text{C}_6\text{H}_{12}$ ):  $\nu(\text{CO})$  2090 w, 2067 m, 2042 m, 1999 vs, 1984 m, 1966 w  $\text{cm}^{-1}$ .  $^1\text{H}$  NMR ( $\text{CDCl}_3$ ):  $\delta$  5.11 (m,  $\text{H}_a$ ), 4.30 (dt,  $\text{H}_b$ ),  $-15.24$  (s, br,  $\text{H}_c$ ),  $-20.83$  (m,  $\text{H}_d$ ),  $J_{aP}$  2.5 Hz,  $J_{ab}$  6.5 Hz,  $J_{ac}$  2.5 Hz,  $J_{ad}$  2.0 Hz,  $J_{bP}$  2.5 Hz,  $J_{bc}$  0.5 Hz,  $J_{bd}$  2.5 Hz,  $J_{cP}$  0.5 Hz,  $J_{cd}$  1.5 Hz,  $J_{dP}$  9.5 Hz;  $\text{P}(\text{C}_6\text{H}_{11})_3$ , several multiplets  $\delta$  1.8–1.5.

**Synthesis of  $(\mu\text{-H})_3\text{Os}_3(\text{CO})_8(\text{PPh}_3)(\mu\text{-CH})$  (7).** A toluene solution of **4** (15 mg, 0.014 mmol) was heated to reflux for 10 h. The bright yellow solution lightened to pale yellow during this period. The reaction mixture was then cooled to room temperature, the solvent was removed under reduced pressure,

(5) (a) Adams, R. D.; Selegue, J. P. *J. Organomet. Chem.* **1980**, *195*, 223. (b) Adams, R. D.; Golembeski, N. M.; Selegue, J. P. *J. Am. Chem. Soc.* **1981**, *103*, 546. (c) Adams, R. D.; Golembeski, N. M.; Selegue, J. P. *Inorg. Chem.* **1981**, *20*, 1242. (d) Adams, R. D.; Katahira, D. A.; Yang, L.-W. *J. Organomet. Chem.* **1981**, *219*, 85. (e) Brown, S. C.; Evans, J. *J. Chem. Soc., Dalton Trans.* **1982**, 1049. (f) Deeming, A. J.; Manning, P. J.; Rothwell, I. P.; Hursthouse, M. B.; Walker, N. P. C. *J. Chem. Soc., Dalton Trans.* **1984**, 2039. (g) Burgess, K.; Holden, H. D.; Johnson, B. F. G.; Lewis, J.; Hursthouse, M. B.; Walker, N. P. C.; Deeming, A. J.; Manning, P. J.; Peters, R. *J. Chem. Soc., Dalton Trans.* **1985**, 85. (h) Deeming, A. J.; Fuchita, Y.; Hardcastle, K.; Henrick, K.; McPartlin, M. *J. Chem. Soc., Dalton Trans.* **1986**, 2259. (i) Deeming, A. J.; Donovan-Mtunzi, S.; Kabir, S. E.; Arce, A. J.; De Sanctis, Y. *J. Chem. Soc., Dalton Trans.* **1987**, 1457. (j) Glavee, G. N.; Daniels, L. M.; Angelici, R. J. *Organometallics* **1989**, *8*, 1856. (k) Kabir, S. E.; Rosenberg, E.; Day, M.; Hardcastle, K. I.; Walt, E.; McPhillips, T. *Organometallics* **1995**, *14*, 721.

(6) Grimme, W.; Doering, W. v. E. *Chem. Ber.* **1973**, *106*, 1765.

(7) Deeming, A. J.; Hasso, S. *J. Organomet. Chem.* **1975**, *88*, C21.

(8) Knox, S. A. R.; Koepke, J. W.; Andrews, M. A.; Kaesz, H. D. *J. Am. Chem. Soc.* **1975**, *97*, 3942.

**Table 1. Crystallographic Data for ( $\mu$ -H)<sub>2</sub>Os<sub>3</sub>(CO)<sub>9</sub>(PPh<sub>3</sub>)( $\mu$ -CH<sub>2</sub>) (4a)**

formula	C <sub>28</sub> H <sub>19</sub> O <sub>9</sub> Os <sub>3</sub> P
fw	1101.00
cryst syst	monoclinic
space group	<i>P</i> 2 <sub>1</sub> / <i>n</i>
<i>a</i> (Å)	9.4856(1)
<i>b</i> (Å)	14.0171(2)
<i>c</i> (Å)	22.4979(4)
$\beta$ (deg)	101.632(1)
<i>V</i> (Å <sup>3</sup> )	2992.90(7)
<i>Z</i>	4
wavelength (Å)	0.710 73
$\rho_c$ (g/cm <sup>3</sup> )	2.695
$\mu$ (mm <sup>-1</sup> )	13.113
no. of rflns collected	18 871
no. of indep rflns	7009
<i>R</i> <sub>int</sub>	0.0453
<i>R</i> 1 [ <i>I</i> > 2 $\sigma$ ( <i>I</i> )] <sup>a</sup>	0.0291
<i>wR</i> 2 <sup>b</sup>	0.0687

$$^a R1 = \sum |F_o - F_c| / \sum |F_o|, \quad ^b wR2 = \{ \sum [w(F_o^2 - F_c^2)^2] / \sum w(F_o^2)^2 \}^{1/2}.$$

and the residue was separated by preparative-scale TLC (SiO<sub>2</sub>, petroleum ether). Two bands were observed. The first band that eluted was yellow and was comprised of the starting compound **4**. The second band was colorless. Extraction with dichloromethane and evaporation of the solvent yielded **7** as an off-white powder (10 mg, 0.0093 mmol, 66%). Anal. Calcd for C<sub>27</sub>H<sub>19</sub>O<sub>8</sub>Os<sub>3</sub>P: C, 30.22; H, 1.78. Found: C, 30.08; H, 1.97. IR (C<sub>6</sub>H<sub>12</sub>):  $\nu$ (CO) 2094 m, 2072 s, 2048 w, 2027 s, 2008 s, 2002 s, 1994 sh, 1961 br cm<sup>-1</sup>. <sup>1</sup>H NMR (CDCl<sub>3</sub>): **7**,  $\delta$  9.83 (s, CH), -18.49 (d, 2H, *J*<sub>HP</sub> 10 Hz), -19.58 (s, 1H); P(C<sub>6</sub>H<sub>5</sub>)<sub>3</sub>,  $\delta$  7.3 (m) and 7.5 (m).

**Protonation of 4a and 6a with HO<sub>2</sub>CCF<sub>3</sub> and DO<sub>2</sub>CCF<sub>3</sub>.** A 10 mg sample of ( $\mu$ -H)<sub>2</sub>Os<sub>3</sub>(CO)<sub>9</sub>L(CH<sub>2</sub>) (L = PPh<sub>3</sub>, PCy<sub>3</sub>) was dissolved in 1 mL of CD<sub>2</sub>Cl<sub>2</sub>, and the solution was transferred to an NMR tube. The tube was cooled to -35 °C in the spectrometer and momentarily ejected, and 15  $\mu$ L of the acid was added. The sample was inserted back into the spectrometer, and the <sup>1</sup>H and <sup>13</sup>C NMR spectra were acquired.

**Reaction of 2, 4, and 6 with Ethylene.** A 250 mL pressure bottle was charged with 35 mL of a hexane solution of **4** (15 mg, 0.014 mmol) and then pressurized to 20 psig with ethylene. The reaction mixture was stirred at room temperature for 24 h. The pressure bottle was then vented, and the solvent was removed under reduced pressure. The residue was dissolved in CDCl<sub>3</sub>, and a <sup>1</sup>H NMR spectrum was taken. This indicated that only 30% of the starting material had reacted with ethylene to form the expected vinyl compound ( $\mu$ -H)Os<sub>3</sub>(CO)<sub>9</sub>(PPh<sub>3</sub>)( $\mu$ , $\eta^2$ -CHCH<sub>2</sub>). Similar reaction conditions were employed for **2** (ca. 100%) and **6** (0%).

**Crystallographic Study of 4a.** Single crystals of ( $\mu$ -H)<sub>2</sub>Os<sub>3</sub>(CO)<sub>9</sub>(PPh<sub>3</sub>)( $\mu$ -CH<sub>2</sub>), grown from a concentrated diethyl ether solution at -20 °C, were mounted on glass fibers with Paratone-N oil (Exxon) and immediately cooled to -75 °C in a cold nitrogen gas stream on a Siemens Platform/CCD automated diffractometer. Standard peak search and indexing procedures gave rough cell dimensions, and least-squares refinement using 7007 reflections yielded the cell dimensions. The systematic absences observed in the diffraction data were consistent only with space group *P*2<sub>1</sub>/*n*. The measured intensities were reduced to structure factor amplitudes by correction for background and Lorentz and polarization effects. Corrections for crystal decay were unnecessary. Absorption effects were corrected analytically, the maximum and minimum transmission factors being 0.777 75 and 0.142 74. Symmetry-equivalent reflections were averaged to yield the set of unique data. All 7007 reflections were used in the least-squares refinement. A summary of crystallographic data for ( $\mu$ -H)<sub>2</sub>Os<sub>3</sub>(CO)<sub>9</sub>(PPh<sub>3</sub>)( $\mu$ -CH<sub>2</sub>) is given in Table 1.

The structure was solved by using direct methods.<sup>9</sup> The full-matrix least-squares refinement (SHELXL-93) was based on

**Table 2. Comparison of Selected Bond Distances (Å) in ( $\mu$ -H)<sub>2</sub>Os<sub>3</sub>(CO)<sub>9</sub>(PPh<sub>3</sub>)( $\mu$ -CH<sub>2</sub>) (4a) and ( $\mu$ -H)<sub>2</sub>Os<sub>3</sub>(CO)<sub>10</sub>( $\mu$ -CH<sub>2</sub>) (1a)**

	4a	1a
Os(1)–Os(2)	2.8226(3)	2.824(3)
Os(1)–Os(3)	3.0808(3)	3.053(3)
Os(2)–Os(3)	2.8694(3)	2.855(3)
Os(1)–C(11)	2.140(6)	2.151(5)
Os(2)–C(11)	2.171(6)	2.150(6)
Os(1)–C(1)	1.902(6)	1.891(4)
Os(1)–C(2)	1.901(7)	1.912(6)
Os(1)–C(3)	1.978(6)	1.949(6)
Os(2)–C(4)	1.905(6)	1.916(4)
Os(2)–C(5)	1.906(6)	1.903(6)
Os(2)–C(6)	1.954(6)	1.933(6)
Os(3)–C(7)	1.901(6)	1.927(4)
Os(3)–P/C(8)	2.386(1)	1.941(4)
Os(3)–C(9)	1.955(6)	1.958(7)
Os(3)–C(10)	1.955(6)	1.966(6)
Os(1)–H(3)	1.83(7)	1.883(9)
Os(3)–H(3)	1.72(7)	1.754(8)
Os(1)–H(4)	1.88(7)	1.834(11)
Os(2)–H(4)	1.80(7)	1.808(10)
C(11)–H(1)	0.96(7)	1.090(11)
C(11)–H(2)	0.94(6)	1.091(10)

*F*<sup>2</sup>.<sup>10</sup> Analytical approximations to the scattering factors were used, and all structure factors were corrected for both real and imaginary components of anomalous dispersion. In the final cycle of least squares, independent anisotropic displacement factors were refined for the non-hydrogen atoms. The methylene hydrogen atoms and the two hydride ligands were located in the difference Fourier map, and their locations were independently refined with individual isotropic displacement factors. An extinction parameter was refined to a final value of  $x = 1.7 \times 10^{-3}$ , where  $F_c$  is multiplied by the factor  $k[1 + F_c^2 x^3 / \sin 2\theta]^{-1/4}$ , with  $k$  being the overall scale factor. Successful convergence was indicated by the maximum shift/error of 0.001 for the last cycle. The largest peak in the final Fourier difference map (1.822 e/Å<sup>3</sup>) was located 0.955 Å from Os(2). A final analysis of variance between observed and calculated structure factors showed no apparent errors. Selected bond distances and angles are displayed in Tables 2 and 3, respectively, and a complete description of the crystallographic results is available as Supporting Information.

**Kinetic Studies of Diazomethane Decomposition.** In a typical experiment 5 mL of a 0.4 M diethyl ether solution of diazomethane was added to a test tube containing a stir bar. The tube was sealed with a rubber septum and then placed in a water bath at 23 °C. One end of a length of plastic tubing was inserted into the open end of a graduated buret that had been filled with water and inverted into the water bath; the other end of the tubing terminated in a syringe needle that was inserted through the septum on the test tube. The compound of interest (ca. 30 mg) was dissolved in 2 mL of diethyl ether, and the resulting solution was injected into the stirred diazomethane solution. Gas (presumed to be nitrogen) evolution was smooth and continuous, and the volume of gas evolved was measured by the change in water level in the buret as a function of time until no further change was observed. Rate constants were derived from the slopes of plots of  $\ln\{V_\infty / (V_\infty - V_t)\}$  vs time, which were linear for at least 4 half-lives. Typically, three separate runs were conducted with each compound, and the rate values were averaged. The results for the various compounds examined are summarized in Table 6.

## Results

**Synthesis of Compounds 2–6.** Achieving satisfactory yields of the phosphine-substituted compounds Os<sub>3</sub>–

(9) Sheldrick, G. M. *Acta Crystallogr.* **1990**, A46, 467.

(10) Sheldrick, G. M. SHELXTL PC, Version 5.0; Siemens Industrial Automation, Inc., Madison, WI, 1994.

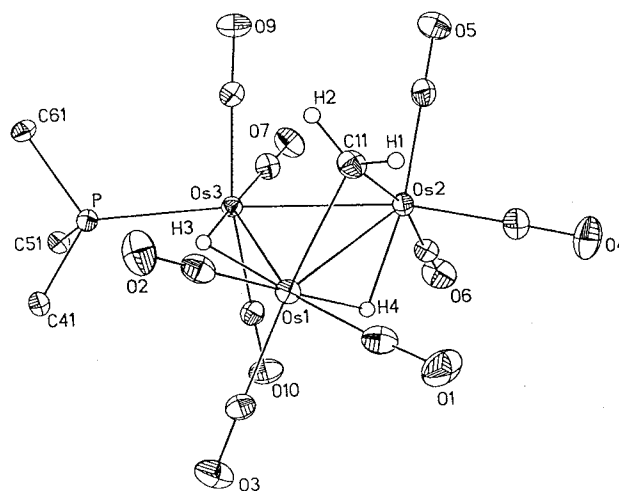


**Table 3.** Comparison of Selected Bond Angles (deg) in  $(\mu\text{-H})_2\text{Os}_3(\text{CO})_9(\text{PPh}_3)(\mu\text{-CH}_2)$  (**4a**) and  $(\mu\text{-H})_2\text{Os}_3(\text{CO})_{10}(\mu\text{-CH}_2)$  (**1a**)

	<b>4a</b>	<b>1a</b>
(A) Angles about Os(1)		
Os(2)–Os(1)–Os(3)	57.965(7)	57.96(7)
Os(2)–Os(1)–C(1)	97.4(2)	98.3(1)
Os(2)–Os(1)–C(2)	140.1(2)	136.6(2)
Os(2)–Os(1)–C(3)	122.2(2)	125.0(2)
Os(2)–Os(1)–C(11)	49.6(2)	48.9(1)
Os(3)–Os(1)–C(11)	79.6(2)	79.8(2)
Os(3)–Os(1)–C(1)	154.8(2)	155.8(2)
Os(3)–Os(1)–C(2)	109.3(2)	108.3(2)
Os(3)–Os(1)–C(3)	95.6(2)	98.0(2)
C(11)–Os(1)–C(1)	87.8(3)	88.0(2)
C(11)–Os(1)–C(2)	92.8(2)	89.9(2)
C(11)–Os(1)–C(3)	171.7(2)	173.8(2)
C(1)–Os(1)–C(2)	92.9(3)	92.3(2)
C(1)–Os(1)–C(3)	94.1(3)	91.9(2)
C(2)–Os(1)–C(3)	95.2(3)	96.3(2)
(B) Angles about Os(2)		
Os(1)–Os(2)–Os(3)	65.532(8)	65.04(8)
Os(1)–Os(2)–C(4)	101.8(2)	103.2(1)
Os(1)–Os(2)–C(5)	134.0(2)	134.6(2)
Os(1)–Os(2)–C(6)	120.8(2)	122.6(2)
Os(1)–Os(2)–C(11)	48.6(2)	49.0(1)
Os(3)–Os(2)–C(11)	84.2(2)	84.6(2)
Os(3)–Os(2)–C(4)	166.8(2)	167.8(2)
Os(3)–Os(2)–C(5)	96.5(2)	95.0(2)
Os(3)–Os(2)–C(6)	87.7(2)	91.2(2)
C(11)–Os(2)–C(4)	89.9(3)	89.6(2)
C(11)–Os(2)–C(5)	89.6(2)	91.0(2)
C(11)–Os(2)–C(6)	168.9(2)	171.6(2)
C(4)–Os(2)–C(5)	95.3(3)	95.8(2)
C(4)–Os(2)–C(6)	96.4(3)	93.2(3)
C(5)–Os(2)–C(6)	98.8(3)	96.6(2)
(C) Angles about Os(3)		
Os(1)–Os(3)–Os(2)	56.503(7)	57.00(7)
Os(1)–Os(3)–C(7)	145.4(2)	141.7(2)
Os(1)–Os(3)–P/C(8)	109.85(4)	118.8(1)
Os(1)–Os(3)–C(9)	95.5(2)	92.0(2)
Os(1)–Os(3)–C(10)	81.2(2)	81.6(2)
Os(2)–Os(3)–C(7)	89.8(2)	85.0(1)
Os(2)–Os(3)–P/C(8)	166.20(4)	175.0(2)
Os(2)–Os(3)–C(9)	82.7(2)	88.4(2)
Os(2)–Os(3)–C(10)	87.6(2)	83.8(2)
C(7)–Os(3)–P/C(8)	104.01(2)	98.9(2)
C(7)–Os(3)–C(9)	87.0(3)	91.4(3)
C(7)–Os(3)–C(10)	90.5(3)	90.5(3)
P/C(8)–Os(3)–C(9)	97.7(2)	94.5(3)
P/C(8)–Os(3)–C(10)	92.4(2)	93.0(3)
C(9)–Os(3)–C(10)	169.9(2)	171.8(2)
(D) Angle at Bridging Methylene Carbon		
Os(1)–C(11)–Os(2)	81.8(2)	82.1(2)

$(\text{CO})_9\text{L}(\text{CH}_4)$  (**2–6**) is more dependent upon specific reaction conditions than in the case of the unsubstituted analogue **1**, which is formed in nearly quantitative yield at room temperature.<sup>1</sup> Yields of the substituted compounds are optimized by using dilute solutions of the dihydride reactant, adding the ethereal diazomethane slowly, and carrying out the reaction at  $-78^\circ\text{C}$ . All of these reaction conditions reduce the amount of hydrocarbon polymer that is formed from the decomposition of diazomethane (vide infra). It is worth noting that the substituted compounds **2–6** appear to be more stable than **1** under ordinary conditions in solution.

**Crystal Structure of 4a.** An ORTEP diagram of **4a** is shown in Figure 1. A triangular array of osmium atoms has the methylene moiety bridging the Os(1)–Os(2) edge, and each of these osmium atoms has three terminal carbonyl ligands. The third osmium atom, Os(3), has four terminal ligands, three carbonyls, and

**Figure 1.** Structural diagram of  $(\mu\text{-H})_2\text{Os}_3(\text{CO})_9(\text{PPh}_3)(\mu\text{-CH}_2)$  (**4a**).

the triphenylphosphine ligand located in an “in-plane” position. This presence of the  $\text{PPh}_3$  ligand on the  $\text{OsL}_4$  center is in contrast to its position in the starting cluster  $(\mu\text{-H})_2\text{Os}_3(\text{CO})_9(\text{PPh}_3)$ , where it is part of an  $\text{OsL}_3$  center flanking the two bridging hydride ligands and the  $\text{OsL}_4$  center has only carbonyl ligands.<sup>11</sup> Both methylene hydrogen atoms and both hydride ligands were located and refined. One hydride ligand bridges the same edge as the methylene ligand, with the methylene above and the hydride below the triosmium plane. The other hydride ligand bridges the Os(1)–Os(3) edge within the triosmium plane, which places it in a cis position relative to the location of the triphenylphosphine ligand.

The overall arrangement of ligands in **4a** is the same as in the unsubstituted analogue **1a**;<sup>2</sup> therefore, a detailed comparison of the structural effects induced by substitution of a carbonyl ligand by the much bulkier triphenylphosphine ligand is of interest. Selected bond distances and angles from the structural studies of **4a** and **1a** are compared in Tables 2 and 3, respectively. The data listed for **1a** are from a neutron diffraction study;<sup>2a</sup> thus, the uncertainties associated with the hydrogen atom positions are an order of magnitude better than those derived from the X-ray data collected for **4a**. Nevertheless, the uncertainties for the carbon atom positions are quite comparable in the two studies, and the specific esd's for the osmium–osmium distances are an order of magnitude better in the X-ray study.

In general, the structural effects induced by the phosphine ligand are rather small and are in the directions expected. The Os(1)–Os(2) vector bridged by both the methylene ligand and the hydride ligand is unchanged in **4a** relative to **1a** (2.8226(3) vs 2.824(3) Å), whereas both the singly bridged Os(1)–Os(3) (3.0808(3) vs 3.053(3) Å) and the unbridged Os(2)–Os(3) (2.8694(3) vs 2.855(3) Å) distances involving the substituted center are slightly longer. The angular distortions around Os(3) in **4a** compared to **1a** occur primarily at the in-plane positions, with the Os(1)–Os(3)–P angle significantly smaller than the corresponding Os(1)–Os(3)–C(8) angle (109.85(4) vs 118.8(1)°), P–Os(3)–C(7) larger than C(8)–Os(3)–C(7) (104.0(2) vs 98.9(2)°), and C(7)–Os(3)–Os(2) also larger (89.8(2) vs 85.0(1)°). How-

(11) Churchill, M. R.; DeBoer, B. G. *Inorg. Chem.* **1977**, *16*, 2397.

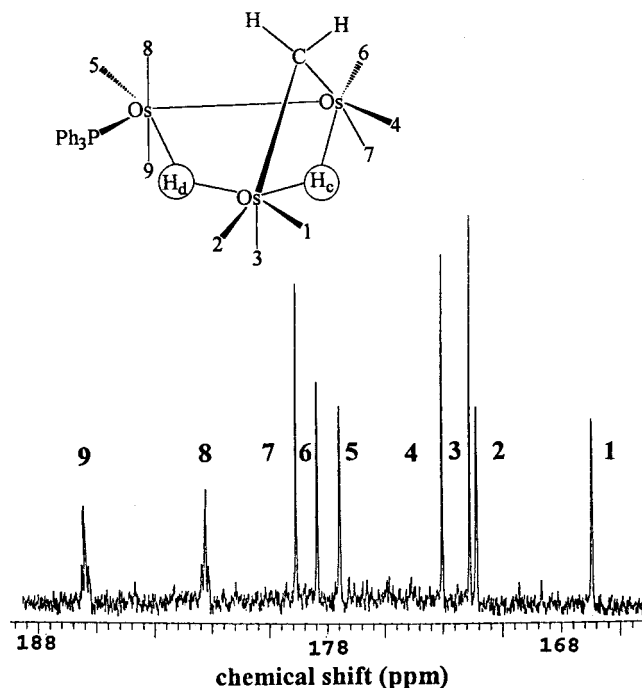


**Figure 2.**  $^{13}\text{C}\{^1\text{H}\}$  NMR spectrum (carbonyl region) of **4a**.

ever, there is some obvious distortion in the position of the out-of-plane carbonyl on the same side as the methylene, as evidenced by the changes in angles Os(1)–Os(3)–C(9) (95.5(2) vs 92.0(2) $^\circ$ ), Os(2)–Os(3)–C(9) (82.7(2) vs 88.4(2) $^\circ$ ), and C(7)–Os(3)–C(9) (87.0(3) vs 91.4(3) $^\circ$ ). The angular distortions around Os(1) are generally small and those around Os(2) even smaller. Perhaps the most interesting change is that the methylene bridge is slightly unsymmetrical in **4a** (Os(1)–C(11) = 2.140(6) Å, Os(2)–C(11) = 2.171(6) Å), with the bridging carbon slightly closer to the side with the phosphine ligand.

**Solution Structures of 4a and Related Methylene Compounds.** The  $^1\text{H}$  NMR spectrum of **4a** in chloroform- $d$  at 20  $^\circ\text{C}$  displays for the methylene ligand a multiplet at  $\delta$  5.08 and a doublet of triplets at  $\delta$  4.26 together with a broad singlet at  $\delta$  –15.37 and a broadened doublet at  $\delta$  –20.18 for the hydride ligands. The same set of signals is seen in the spectrum of **1a**,<sup>1b</sup> and spectra of each of the other methylene derivatives show strictly analogous signals together with appropriate ligand resonances. Homonuclear proton decoupling experiments have been used to obtain the coupling constants listed in the Experimental Section. By analogy with detailed studies of assignments for **1a**,<sup>12</sup> the higher field hydride signal is due to the single hydrogen bridge (supported by the observation of ca. 10 Hz coupling to the  $^{31}\text{P}$  nucleus), the lower field hydride signal to the hydrogen bridge accompanying the methylene bridge, the signal near  $\delta$  5.1 to the methylene proton oriented over the Os $_3$  triangle, and the signal near  $\delta$  4.3 to its counterpart oriented away from the metal core.

The  $^{13}\text{C}\{^1\text{H}\}$  NMR spectrum of  $^{13}\text{CO}$ -enriched **4a** is shown in Figure 2. Assignments for the resonances of the carbonyl ligands are shown by the diagram in Figure 2 and the list given in Table 4. These assignments are

**Table 4.**  $^{13}\text{C}$  NMR Data for ( $\mu$ -H) $_2$ Os $_3$ (CO) $_9$ (PPh $_3$ )( $\mu$ -CH $_2$ ) (**4a**)

peak	$\delta$	$J(\text{C}-\text{H}_c)$ (Hz)	$J(\text{C}-\text{H}_d)$ (Hz)	$J(\text{C}-\text{P})$ (Hz)
1	167.12	1.0	8.5	
2	171.56	11	2.7	
3	171.84	1.5	3.8	
4	172.92	3.8	2	1.0
5	176.88	1.5	3	3.0
6	177.76	8.5		
7	178.58			
8	181.15		3	5.0
9	186.66		3	5.0
CH $_2$	25.52			

made on the basis of criteria also used in previous detailed studies of **1a**<sup>12</sup> and of the related ethylidene compound ( $\mu$ -H) $_2$ Os $_3$ (CO) $_9$ (PPh $_3$ )( $\mu$ -CHCH $_3$ ).<sup>13</sup> (1) The most downfield resonances, 8 and 9, show triplet patterns due to a relatively large value of  $J(^{13}\text{C}-^{13}\text{C})$  characteristic of *trans* carbonyl ligands on an OsL $_4$  moiety.<sup>14</sup> (2) Resonances 9, 8, and 5 show significant values of  $J(^{13}\text{C}-^{31}\text{P})$ , indicating that these signals are due to the three carbonyls on the same osmium center as the phosphine ligand. These signals are shifted downfield 8–9 ppm compared to signals for carbonyls in the same positions in unsubstituted **1a**. (3) Selective decoupling experiments show that resonances 2 and 6 both show strong coupling to H $_c$ , and resonance 1 shows strong coupling to H $_d$ , which indicates that the corresponding carbonyls are located *trans* with respect to the specific hydride ligands.<sup>15–17</sup> Resonance 2 shows a small but significant coupling to H $_d$ , and resonance 3 shows coupling to both H $_c$  and H $_d$ ; therefore resonances 1, 2, and 3 correspond to three carbonyls on the same osmium center. (4) Resonance 4 shows a small  $^{31}\text{P}$  coupling that suggests the corresponding carbonyl is in a position *trans* to the metal–metal bond leading to the substituted osmium center. This leaves only resonance 7, which is assigned to the final carbonyl ligand on the second OsL $_3$  unit.

The solution structure of the ethylidene compound ( $\mu$ -H) $_2$ Os $_3$ (CO) $_9$ (PPh $_3$ )( $\mu$ -CHCH $_3$ ) was deduced previously by analyzing  $^{13}\text{C}-^{13}\text{C}$  as well as  $^{13}\text{C}-^1\text{H}$  couplings.<sup>13</sup> Both the  $^1\text{H}$  and  $^{13}\text{C}$  NMR spectra of the ethylidene compound are very closely analogous to those for the methylene compound **4a**. In neither case is the relative placement of the phosphine ligand and the in-plane carbonyl ligand on the OsL $_4$  unit unambiguously established by the spectroscopic data alone. However, given the solid-state structure determined for **4a**, in which the single hydride bridge is *cis* to the phosphine ligand, it is most likely that this configuration is maintained in solution not only for **4a** but for the ethylidene compound as well.

**NMR Spectroscopic Characterization of Methyl Tautomers.** The  $^1\text{H}$  NMR spectrum of a solution

(13) Koike, M.; Shapley, J. R. *J. Organomet. Chem.* **1994**, 470, 199.

(14) (a) Tachikawa, M.; Richter, S. I.; Shapley, J. R. *J. Organomet. Chem.* **1977**, 123, C9. (b) Clauss, A. D.; Tachikawa, M.; Shapley, J. R. *Inorg. Chem.* **1981**, 20, 1528.

(15) (a) Farrugia, L. J. *J. Organomet. Chem.* **1990**, 394, 515. (b) Ewing, P.; Farrugia, L. J. *Organometallics* **1989**, 8, 1246. (c) Ewing, P.; Farrugia, L. J. *Organometallics* **1989**, 8, 1665. (d) Ewing, P.; Farrugia, L. J. *Organometallics* **1988**, 7, 871. (e) Ewing, P.; Farrugia, L. J. *Organometallics* **1988**, 7, 859.

(16) Keister, J. B.; Shapley, J. R. *Inorg. Chem.* **1982**, 21, 3304.

(17) Aime, S.; Osella, L.; Milone, L.; Rosenberg, E. *J. Organomet. Chem.* **1981**, 213, 207.

(12) Koike, M.; VanderVelde, D. G.; Shapley, J. R. *Organometallics* **1994**, 13, 1404.

**Table 5. Influence of the Phosphine Ligand on the Tautomer Equilibrium for  $\text{Os}_3(\text{CO})_9(\text{L})(\text{CH}_4)$** 

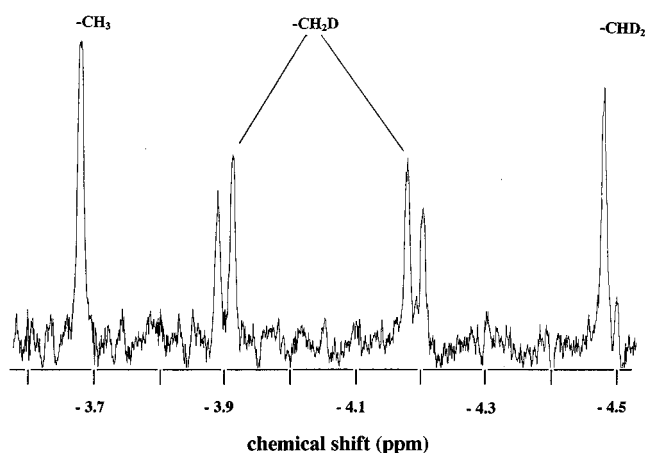
compd	ligand	cone angle (deg) <sup>a</sup>	$\text{p}K_{\text{a}}^a$	$K_{\text{eq}}^b$
1	CO			3
2	$\text{PEt}_3$	132	8.69	12
3	$\text{PET}_2\text{Ph}$	136	6.25	30
4	$\text{PPh}_3$	145	2.73	56
5	$\text{PiPrPh}_2$	151		130
6	$\text{PCy}_3$	162	9.70	>200 <sup>c</sup>

<sup>a</sup> Data from refs 18 and 19. <sup>b</sup> Refers to the ratio of methylene to methyl compounds. <sup>c</sup> Methyl tautomer could not be detected by  $^1\text{H}$  NMR.

prepared from isolated methylene compound **4a** also contains weak signals appropriate for the methyl isomer **4b**, a broad singlet at  $\delta$  -3.68 (3H) for the methyl group, and a doublet of quartets at  $\delta$  -14.79 (1H) for the hydride ligand. Selective decoupling experiments reveal that the methyl and hydride signals are mutually coupled ( $J_{\text{HH}} = 1$  Hz), and each is coupled to the  $^{31}\text{P}$  nucleus. The positions of these signals are closely similar to those seen for unsubstituted **1b**.<sup>1</sup> Analogous signals are seen in the spectra of the derivatives **2a**–**5a** but could not be detected in the spectrum of **6a**. The relative intensity of the methyl isomer signals varies with the specific phosphine ligand, and the observed ratios are summarized in Table 5 together with appropriate ligand data. The relative concentration of the methyl isomer decreases with increasing cone angle of the phosphine ligand.<sup>18</sup> This ratio appears to be independent of the electronic properties of the ligand, since  $\text{PEt}_3$  and  $\text{PCy}_3$  have similar electronic properties<sup>19</sup> but show very different values of the methyl-to-methylene ratio in compounds **2** and **6**.

An equilibrium between the two isomers was established by dissolving crystals of **4a** and then monitoring the  $^1\text{H}$  NMR spectrum. Initially, only signals due to the methylene tautomer were detected, but signals for the methyl tautomer gradually appeared until an equilibrium ratio of 56:1 was attained. The system reached equilibrium after 45 min. Assuming that this represents 5 half-lives, a rough half-life of 10 min can be estimated, which results in the rate constants  $k_1 = 0.001 \text{ min}^{-1}$  and  $k_2 = 0.07 \text{ min}^{-1}$ . Although the errors associated with these numbers are admittedly large, the values obtained are comparable with the rate constants ( $k_1 = 0.0026 \text{ min}^{-1}$ ,  $k_2 = 0.0058 \text{ min}^{-1}$ ) determined for interconversion of the two isomers of  $(\mu\text{-H})\text{Os}_3(\text{CO})_9(\text{PPh}_3)(\mu, \eta^2\text{-CH=CH}_2)$ .<sup>20</sup>

We have also observed that there is considerably more methyl tautomer present in the crude reaction mixture than in the equilibrium mixture. The methyl/methylene tautomerization appears to be catalyzed by silica gel, since the equilibrium ratio is immediately established after purification by preparative thin-layer chromatography (TLC). Isotopic exchange of hydrogen for deuterium under these conditions has been demonstrated for the unsubstituted compounds **1a/1b**,<sup>1c</sup> and these processes are likely related to the propensity to protonation demonstrated for the methylene tautomers (vide infra).

**Figure 3.**  $^1\text{H}$  NMR signals for the methyl group in **4b-d**<sub>2</sub> (18 °C,  $\text{CDCl}_3$ ).

The upfield shift of the methyl resonance can be attributed to a time-averaged signal for two protons in a normal C–H bond and one proton in an “agostic”<sup>21</sup> three-center, two-electron  $\text{C}\cdots\text{H}\cdots\text{Os}$  bond, as characterized previously for the unsubstituted methyl compound **1b**.<sup>1a</sup> Lowering the temperature causes significant broadening of the methyl signal for **4a**; in fact, the signal broadens into the baseline at -85 °C. We attribute this broadening to slow rotation of the methyl group, which interconverts the terminal and bridging hydrogen atoms. Unfortunately, even at -125 °C we did not see separate signals for the terminal and bridging protons of the methyl group, which would allow us to calculate an exchange rate. It is interesting to note that no broadening was observed for **1b** down to -100 °C.<sup>1a</sup>

A deuterium labeling study was undertaken to confirm the unsymmetrical bridging mode of the methyl group, as was done previously for **1b**.<sup>1a</sup> When the reaction with diazomethane is carried out with  $(\mu\text{-D})_2\text{Os}_3(\text{CO})_9\text{PPh}_3$ , the resulting  $\text{Os}_3(\text{CO})_9(\text{PPh}_3)(\text{CH}_2\text{D}_2)$  product shows four signals in the methyl region of the  $^1\text{H}$  NMR spectrum (see Figure 3). The first signal is due to the “ $\text{CH}_3$ ” isotopomer that results from partial loss of the deuterium label. The next two signals are an AB quartet, as established by homonuclear decoupling experiments, due to the two inequivalent protons in the “ $\text{CH}_2\text{D}$ ” isotopomer, and the fourth signal is a broad singlet due to the “ $\text{CHD}_2$ ” isotopomer. The unsubstituted compound **1b** shows time-averaged mirror symmetry that relates the two protons in the “ $\text{CH}_2\text{D}$ ” isotopomer;<sup>12</sup> therefore, only three methyl signals overall are seen.<sup>1a</sup> However, in **4b** the presence of the phosphine ligand removes the possibility of achieving such symmetry, with the result that the two protons in the “ $\text{CH}_2\text{D}$ ” isotopomer appear spectroscopically distinct.

When the temperature of a sample of **4-d**<sub>2</sub> is lowered, the separation between the methyl signals for the three isotopomers (taking an average value for the “ $\text{CH}_2\text{D}$ ” isotopomer) increases. Figure 4 shows a plot of  $\Delta_1$  (separation between “ $\text{CH}_3$ ” and “ $\text{CH}_2\text{D}$ ”) and  $\Delta_2$  (separation of “ $\text{CH}_2\text{D}$ ” and “ $\text{CHD}_2$ ”) vs  $1/T$  for both **4-d**<sub>2</sub> and unsubstituted **1-d**<sub>2</sub>. Both  $\Delta_1$  and  $\Delta_2$  increase as the temperature is decreased, and  $\Delta_2$  increases more than

(18) Tolman, C. A. *Chem. Rev.* **1977**, *77*, 313.

(19) Rahman, M.; Liu, H. Y.; Prock, A.; Giering, W. P. *Organometallics* **1987**, *6*, 650.

(20) (a) Hamilton, D. H.; Shapley, J. R. *Organometallics* **1998**, *17*, 3087. (b) Koike, M.; Hamilton, D. H.; Wilson, S. R.; Shapley, J. R. *Organometallics* **1996**, *15*, 4930.

(21) (a) Brookhart, M.; Green, M. L. H. *J. Organomet. Chem.* **1983**, *250*, 395. (b) Brookhart, M.; Green, M. L. H.; Wong, L.-L. *Prog. Inorg. Chem.* **1988**, *36*, 1.



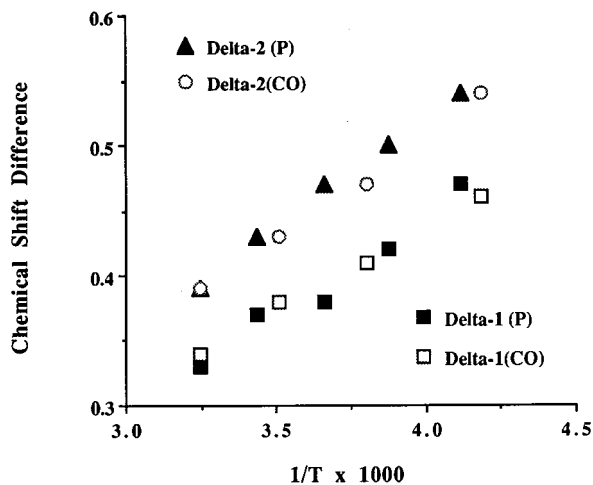
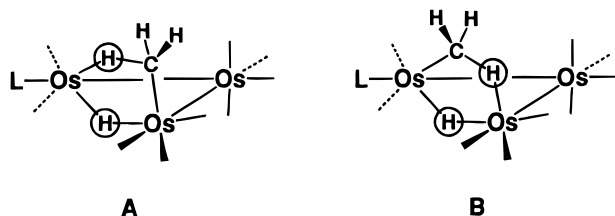


**Figure 4.** Temperature dependence of isotopomer chemical shift differences  $\Delta_1$  ( $\delta(\text{CH}_2\text{D}) - \delta(\text{CH}_3)$ ) and  $\Delta_2$  ( $\delta(\text{CHD}_2) - \delta(\text{CH}_2\text{D})$ ) for **4b-d<sub>2</sub>** and **1b-d<sub>2</sub>**.

**Chart 1**



$\Delta_1$ . Virtually identical results are seen for a sample of **2-d<sub>2</sub>**, with only slight changes in chemical shift. This behavior is uniquely dependent upon an equilibrium isotope effect that favors the heavier isotope in the nonbridging (higher frequency) site.<sup>1a,21–23</sup> Although a recent discussion of this phenomenon in a similar context has pointed out that the same type of spectral behavior is predicted also for a hydrido methylene substructure undergoing rapid equilibration,<sup>24</sup> we think that this is unlikely in the case of **4b**, in particular given the close parallel with **1b** seen in Figure 4.

We propose that the methyl ligand in **4b** and the related compounds is in a bridging position (along with the hydride ligand) that is adjacent to the location of the phosphine ligand, as shown in Chart 1. The evidence for this assignment is as follows. (1) Both the hydride ligand and the protons on the methyl group show significant coupling to the phosphorus nucleus ( $J_{\text{HP}} = 8$  and 2 Hz, respectively). (2) The  $^{31}\text{P}$  chemical shifts for the PPh $_3$  ligand in **4a** and **4b** are significantly different ( $-8.05$  vs  $6.32$  ppm, respectively), and both the difference and direction are consistent with the phosphine ligand being part of an Os(CO) $_3$ L group in **4a** but part of an Os(CO) $_2$ L group in **4b**.<sup>15</sup> (3) The net effect of the phosphine ligand on the chemical shift difference between the two protons in the CH $_2$ D tautomer is larger for **4b** (and **2b**) than for protonated **4a** and **6a**, where the new methyl group is clearly remote from the site of phosphine ligand substitution (vide infra). The two

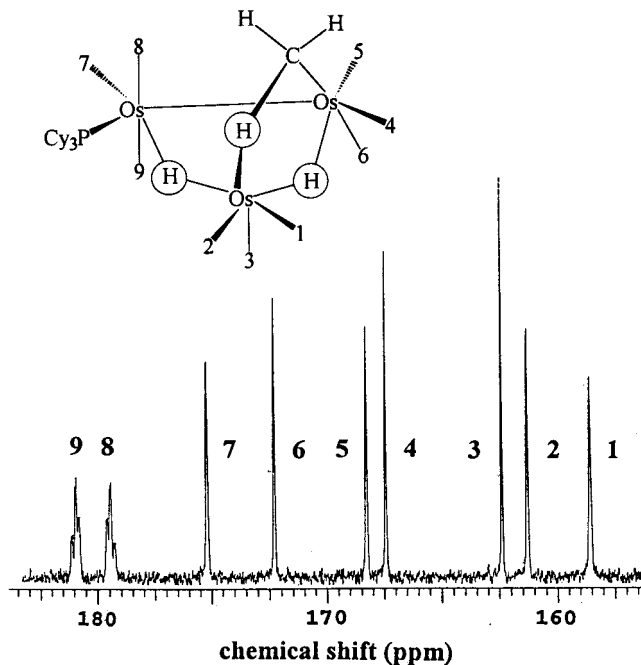


**Figure 5.**  $^{13}\text{C}\{^1\text{H}\}$  NMR spectrum ( $-30^\circ\text{C}$ ,  $\text{CDCl}_3$ , carbonyl region) of  $[(\mu\text{-H})_2\text{Os}_3(\text{CO})_9(\text{PCy}_3)(\mu\text{-CH}_3)][\text{O}_2\text{CCF}_3]$ .

possible configurations shown in Chart 1 differ in whether the agostic interaction is with the substituted osmium center or not. These configurations are degenerate in energy and are rapidly interconverted in the case of unsubstituted **1b**.<sup>13</sup> They differ in energy for **4b** but may still be readily interconvertible, as in the case of the bridging vinyl ligand in the corresponding adjacent isomer of  $(\mu\text{-H})\text{Os}_3(\text{CO})_9(\text{PPh}_3)(\mu,\eta^2\text{-CH=CH}_2)$ .<sup>20b</sup> We suggest that configuration A, with the agostic bridge to the more basic osmium center, is likely to be more stable. The analogous configuration for  $(\mu\text{-H})\text{Os}_3(\text{CO})_9(\text{PPh}_3)(\mu,\eta^2\text{-CH=CH}_2)$  has the  $\pi$  bond of the bridging vinyl group coordinated to the substituted osmium atom.<sup>20b</sup>

**Protonation of  $(\mu\text{-H})_2\text{Os}_3(\text{CO})_9\text{L}(\mu\text{-CH}_2)$ .** Monitoring the addition of trifluoroacetic acid to  $(\mu\text{-H})_2\text{Os}_3(\text{CO})_9(\text{PCy}_3)(\mu\text{-CH}_2)$  at  $-35^\circ\text{C}$  by  $^1\text{H}$  NMR discloses that the signals for the methylene protons disappear immediately, and a new resonance appears at  $\delta -2.85$ . This indicates that the proton adds to a Os–C bond to form a new methyl compound rather than to an Os–Os bond. The two hydride signals shift downfield to  $\delta -19.36$  and  $-14.93$  but are otherwise unchanged. The  $^{13}\text{C}\{^1\text{H}\}$  NMR spectrum of  $[(\mu\text{-H})_2\text{Os}_3(\text{CO})_9(\text{PCy}_3)(\mu\text{-CH}_3)]^+$  is shown in Figure 5. The spectrum is very similar to that of **4a** (Figure 2), indicating that the relative orientation of the ligands is unchanged (i.e., the phosphine ligand is still located on an OsL $_4$  unit). The specific carbonyl assignments shown in the diagram in Figure 5 were deduced by selective proton decoupling and by comparison with the study of **4a**.

The protonation with trifluoroacetic acid has also been carried out with the **4a/4b** mixture at  $-30^\circ\text{C}$ . The proton only adds to the methylene tautomer, **4a**, as evidenced by the retention of the resonance attributable to the methyl group in **4a**, with an intensity of ca. 1:56 relative to that of the new methyl resonance for  $[(\mu\text{-H})_2\text{Os}_3(\text{CO})_9(\text{PPh}_3)(\mu\text{-CH}_3)]^+$ . This selectivity is even more obvious in the protonation of the **1a/1b** mixture,

(22) Green, M. L. H.; Hughes, A. K.; Popham, N. A.; Stephens, A. H. H.; Wong, L.-L. *J. Chem. Soc., Dalton Trans.* **1992**, 3077.

(23) Casey, C. P.; Hallenbeck, S. L.; Widenhoefer, R. A. *J. Am. Chem. Soc.* **1995**, *117*, 4607.

(24) Torkelson, J. R.; Antwi-Nsiah, F. H.; McDonald, R.; Cowie, M.; Pruis, J. G.; Jalkanen, K. J.; DeKock, R. L. *J. Am. Chem. Soc.* **1999**, *121*, 3666.

in which **1a** is converted to a cationic methyl complex and **1b** is unchanged.<sup>1c</sup>

Broadening of the methyl signal as the temperature is lowered is also observed for  $[(\mu\text{-H})_2\text{Os}_3(\text{CO})_9(\text{PCy}_3)(\mu\text{-CH}_3)]^+$  (the signal broadens into the baseline at  $-90^\circ\text{C}$ ). The unsymmetrical nature of the bonding of the methyl group is confirmed by reaction with deuterated trifluoroacetic acid. The new product shows a signal due to  $\text{CH}_3$  and two signals due to  $\text{CH}_2\text{D}$ . It is significant that the separation between the two  $\text{CH}_2\text{D}$  signals is smaller for the protonated compound  $[(\mu\text{-H})_2\text{Os}_3(\text{CO})_9(\text{PCy}_3)(\mu\text{-CH}_2\text{D})]^+$  than in  $(\mu\text{-D})\text{Os}_3(\text{CO})_9(\text{PPh}_3)(\mu\text{-CH}_2\text{D})$  (0.15 ppm vs 0.40 ppm at  $-30^\circ\text{C}$ ), which is consistent with the methyl group being more removed from the influence of the phosphine ligand in the cationic compound. When an excess of acid is used, a signal attributable to  $\text{CHD}_2$  grows in at the expense of the  $\text{CH}_3$  signal, indicating that intermolecular exchange is occurring. Indeed, complete deuteration of the compound can be achieved with sufficient time and excess of acid. The separation between the signals for the three isotopomers (again taking an average signal for the two  $\text{CH}_2\text{D}$  signals) shows a temperature effect similar to that observed for **4b-d**<sub>2</sub>.

A solution of  $[(\mu\text{-H})_2\text{Os}_3(\text{CO})_9(\text{PCy}_3)(\mu\text{-CH}_3)][\text{O}_2\text{CCF}_3]$  is unstable above  $-20^\circ\text{C}$ . The  $^1\text{H}$  NMR spectrum shows relatively clean formation of methane and a hydrido/trifluoroacetate triosmium cluster,  $(\mu\text{-H})\text{Os}_3(\text{CO})_9(\text{PCy}_3)(\mu\text{-O}_2\text{CCF}_3)$ , which can be identified by analogy to the product of protonation of **1a**,  $(\mu\text{-H})\text{Os}_3(\text{CO})_{10}(\mu\text{-O}_2\text{CCF}_3)$ .<sup>1c,25</sup>

**Formation of Methylidyne Compound 7.** Thermolysis of a toluene solution of **4** results in the formation of the triphenylphosphine-substituted methylidyne compound **7**. The reaction proceeds in good yield with only a small amount of decomposition. The methylidyne compound has been identified by its  $^1\text{H}$  NMR spectrum, which contains a low-field resonance at  $\delta$  9.84 attributable to the methylidyne proton and two high-field resonances in a ratio of 2:1 due to the three hydride ligands. The hydride resonance with an intensity of 2 shows coupling to the phosphorus nucleus with a  $J_{\text{HP}}$  value of 10 Hz. This result implies that the phosphine ligand resides in a pseudoaxial position, consistent with the structural assignments made for a variety of related  $\text{M}_3(\text{CO})_8\text{L}(\mu\text{-CX})$  alkylidyne compounds for both  $\text{M} = \text{Ru}$  and  $\text{M} = \text{Os}$ .<sup>26,27</sup>

**Reactions of Tautomeric Mixtures with Ethylene.** A solution of the triethylphosphine derivative **2a/2b**, placed under a pressure of ca. 20 psig of ethylene, shows after 24 h nearly quantitative conversion to the corresponding vinyl compound,  $(\mu\text{-H})\text{Os}_3(\text{CO})_9\text{PET}_3(\mu,\eta^2\text{-CH=CH}_2)$ .<sup>20b</sup> However, under the same conditions with the triphenylphosphine derivative **4a/4b**, ca. 70% of the starting material is recovered, and with the tricyclohexylphosphine-substituted **6a** no reaction occurs. Since the time required for tautomer equilibration, specifically observed in the case of **4b**  $\rightarrow$  **4a**, is much shorter than

**Table 6. Rate Constants for Diazomethane Decomposition**

compd	$k$ ( $\text{min}^{-1}$ )			
	trial 1	trial 2	trial 3	average <sup>a</sup>
$\text{Os}_3(\text{CO})_{10}(\text{CH}_4)$ ( <b>1</b> )	1.3	1.0	1.3	1.2(1)
$\text{Os}_3(\text{CO})_9\text{PET}_3(\text{CH}_4)$ ( <b>2</b> )	0.23	0.23	0.23	0.23(2)
$\text{Os}_3(\text{CO})_9\text{PPh}_3(\text{CH}_4)$ ( <b>4</b> )	0.75	0.84	0.81	0.80(7)
$\text{H}_2\text{Os}_3(\text{CO})_{10}$	1.4	1.1	1.2	1.3(2)
$\text{H}_2\text{Os}_3(\text{CO})_9\text{PET}_3$	0.23	0.24	0.23	0.23(2)
$\text{H}_2\text{Os}_3(\text{CO})_9\text{PPh}_3$	0.77	0.86	0.81	0.81(6)
$\text{H}_2\text{Os}_3(\text{CO})_9\text{P}(\text{C}_6\text{H}_4\text{Me})_3$	0.73	0.69	0.67	0.70(6)
$\text{H}_2\text{Os}_3(\text{CO})_9\text{P}(\text{C}_6\text{H}_4\text{OMe})_3$	0.61	0.55	0.58	0.58(5)
$\text{H}_2\text{Os}_3(\text{CO})_9\text{PCy}_3$	0.25	0.23	0.24	0.24(2)
$\text{HOs}_3(\text{CO})_{10}(\text{CH=CH}_2)$	0.42	0.41	0.44	0.42(4)

<sup>a</sup> Estimated errors at the 95% confidence level are given in parentheses.

the reaction time with ethylene, this ligand effect can be attributed to steric inhibition of ethylene coordination to the methyl complex prior to methane elimination.

**Catalytic Decomposition of Diazomethane.** Rates for the decomposition of excess (ca. 70-fold) diazomethane by **1**, **2**, and **4** as well as related compounds are displayed in Table 6. The rate constants determined for the methyl/methylene tautomers are indistinguishable from those for their  $\text{H}_2\text{Os}_3(\text{CO})_9\text{L}$  precursors, and in each case the rate constants decrease as  $\text{L} = \text{CO} > \text{PPh}_3 > \text{PET}_3$ . The suggestion that this order is determined by the relative donor properties of the ligands is substantiated by the values obtained for additional  $\text{H}_2\text{Os}_3(\text{CO})_9\text{L}$  compounds, which results in the overall order of  $\text{L} = \text{CO} \gg \text{PPh}_3 > \text{P}(\text{C}_6\text{H}_4\text{Me})_3 > \text{P}(\text{C}_6\text{H}_4\text{OMe})_3 \gg \text{PET}_3 \approx \text{PCy}_3$ . The FAB(+) mass spectrum of polymer isolated from the reaction for  $\text{L} = \text{PPh}_3$  showed prominent peaks corresponding to monoalkenes between  $\text{C}_{28}\text{H}_{56}$  and  $\text{C}_{66}\text{H}_{132}$ , with  $\text{C}_{48}\text{H}_{96}$  being the most abundant. This result suggests that the reaction proceeds by generating a long-chain alkyl ligand, which is then released as the alkene following  $\beta$ -hydrogen transfer to the metal catalyst. This idea is consistent with our observation that  $\text{H}_2\text{Os}_3(\text{CO})_9\text{L}$  and  $\text{Os}_3(\text{CO})_9\text{L}(\text{CH}_4)$  were always present in the reaction solutions, regardless of which species was added at the beginning. Also, relatively rapid  $\beta$ -H transfer and release of the alkene has been measured directly for  $\text{HOs}_3(\text{CO})_{10}(\text{CH}_2\text{CH}_3)$ .<sup>4b</sup> It is interesting that the vinyl complex  $\text{HOs}_3(\text{CO})_{10}(\mu\text{-CH=CH}_2)$  also catalyzes diazomethane decomposition, at a rate less than half that of either  $\text{H}_2\text{Os}_3(\text{CO})_{10}$  or **1**. However, it is important to note that the reaction with the vinyl compound showed a short induction period, which was not seen with the other catalysts, and no vinyl compound (unsubstituted or substituted) was isolated from the reaction solutions.

## Discussion

The primary results from this study are to show the existence and interrelationship of a set of phosphine ligand substituted triosmium methyl/methylene/methylidyne clusters that parallels the unsubstituted system previously characterized.<sup>1</sup> The new system is summarized in Scheme 2. The presence of the phosphine ligand is nontrivial, however, in the following four ways. (1) The equilibrium abundance of the two tautomers is dependent upon the specific phosphine ligand, with the methylene/methyl ratio increasing with increasing size

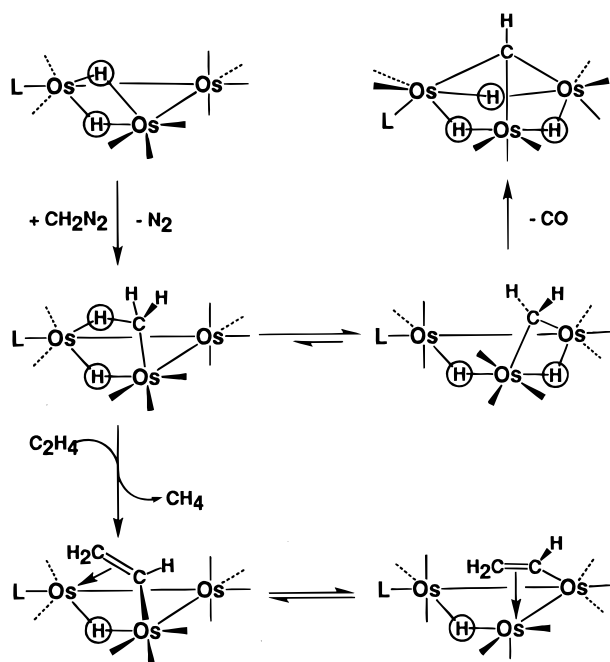
(25) Bryan, E. G.; Johnson, B. F. G.; Lewis, J. J. *Chem. Soc., Dalton Trans.* **1977**, 1328.

(26) (a) Rahman, Z. A.; Beanan, L. R.; Bavaro, L. M.; Modi, S. P.; Keister, J. B.; Churchill, M. R. *J. Organomet. Chem.* **1984**, 263, 75. (b) Feighery, W. G.; Allendoerfer, R. D.; Keister, J. B. *Organometallics* **1990**, 9, 2424.

(27) Johnson, B. F. G.; Lewis, J.; Whitton, A. J. *J. Chem. Soc., Dalton Trans.* **1990**, 3129.



Scheme 2



of the phosphine. An unfavorable steric interaction between the methyl moiety and the adjacent phosphine ligand is relieved by formation of the compound with the methylene ligand remote from the phosphine. This demonstrates mobility for a methyl or methylene ligand on the triosmium framework in response to steric pressure analogous to that previously characterized for a vinyl ligand.<sup>20</sup> (2) Despite the presence of a bulky triphenylphosphine ligand in **4b**, subsequent C–H bond activation in the methylene group occurs to form the substituted methylidyne complex **7**, in higher overall yield than in the unsubstituted case. (3) The ease with which the methyl/methylene tautomers react with typical ligands such as ethylene is greatly affected by the steric bulk of the phosphine ligand present. This is the likely reason the substituted compounds appear more stable in solution than unsubstituted **1**. (4) The activity of the substituted methyl/methylene tautomers as catalysts (or catalyst precursors) for the decomposition of diazomethane depends inversely on the donor character of the substituting ligand. By comparison with (3), this

indicates that the rate-determining step in the reaction with diazomethane is not its coordination to the catalyst. More likely the formation of a new C–C bond is rate-determining, with an indication that the homologating species (probably either  $\eta^1\text{-CH}_2$  or  $\eta^1\text{-CH}_2\text{N}_2$ ) bears some effective positive charge. The involvement of methyl compounds as (pre)catalysts in this system is consistent with an alkyl initiation site, as postulated by Brady and Pettit for their model Fischer–Tropsch system using diazomethane.<sup>28</sup> However, our current results do not eliminate the alternative of vinyl or vinylidene initiation, as proposed by Maitlis and co-workers in their Fischer–Tropsch-related studies,<sup>29</sup> since methane elimination from, for example, **1b** in the presence of diazomethane would give species that we have shown will couple methylenes into vinyl groups.<sup>30</sup> More work with this system will be necessary in order to define the actual nature of the chain-carrying catalyst.

**Acknowledgment.** This work was supported by grants from the National Science Foundation (CHE 9414217) and from the UIUC Campus Research Board. Purchase of the Siemens Platform/CCD diffractometer by the School of Chemical Sciences at the University of Illinois was supported by National Science Foundation Grant No. CHE 9503145. NMR spectra were obtained using instruments in the Varian Oxford Instrument Center for Excellence in NMR laboratory in the School of Chemical Sciences; external funding for this instrumentation was obtained from the Keck Foundation, NIH, and NSF.

**Supporting Information Available:** Details of the crystallographic investigation of compound **4b**, including tables of atomic coordinates and displacement parameters. This material is available free of charge via the Internet at <http://pubs.acs.org>.

OM9904293

(28) (a) Brady, R. C.; Pettit, R. *J. Am. Chem. Soc.* **1980**, *102*, 6181. (b) Brady, R. C.; Pettit, R. *J. Am. Chem. Soc.* **1981**, *103*, 1287.

(29) (a) Turner, M. L.; Long, H. C.; Shenton, A.; Byers, P. K.; Maitlis, P. M. *Eur. J. Chem.* **1995**, *1*, 549. (b) Quyoum, R.; Berdini, V.; Turner, M. L.; Long, H. C.; Maitlis, P. M. *J. Am. Chem. Soc.* **1996**, *118*, 10888. (c) Quyoum, R.; Berdini, V.; Turner, M. L.; Long, H. C.; Maitlis, P. M. *J. Catal.* **1998**, *173*, 355. (d) Mann, B. E.; Turner, M. L.; Quyoum, R.; Marsih, N.; Maitlis, P. M. *J. Am. Chem. Soc.* **1999**, *121*, 6497.

(30) Shapley, J. R.; Sievert, A. C.; Churchill, M. R.; Wasserman, H. J. *J. Am. Chem. Soc.* **1981**, *103*, 6975.